

## the warm-rain season over Eastern Monsoon China

Chenxi Li<sup>1</sup>, Xihui Gu<sup>1,2,3,4,5\*</sup>, Wenkui Bai<sup>6,7</sup>, Louise J. Slater<sup>8</sup>, Jianfeng Li<sup>9</sup>, Dongdong Kong<sup>1</sup>,Jianyu Liu<sup>10, 11\*</sup>, Yanan Li<sup>12, 13</sup>

1. Department of Atmospheric Science, School of Environmental Studies, China University of Geosciences, Wuhan 430074, China;
2. Joint Research Center of National Meteorological Administration on Extreme Weather, Climate and Hydrological Geological Disasters, Wuhan, 430074, China;
3. State Environmental Protection Key Laboratory of Source Apportionment and Control of Aquatic Pollution, Ministry of Ecology and Environment, China;
4. Collaborative Innovation Center for Western Ecological Safety, Lanzhou University, Lanzhou 730000, China;
5. Key Laboratory of Geospatial Technology for Middle and Lower Yellow River Regions (Henan University), Ministry of Education, Kaifeng 475001, China;
6. Pengjiang District Science and Technology Center, Jiangmen 529000, China;
7. Pengjiang District Natural Resources Bureau, Jiangmen 529000, China;
8. School of Geography and the Environment, University of Oxford, Oxford OX1 3QY, UK
9. Department of Geography, Hong Kong Baptist University, Hong Kong, China;
10. Laboratory of Critical Zone Evolution, School of Geography and Information Engineering, China University of Geosciences, Wuhan 430074, China;
11. State Key Laboratory of Loess and Quaternary Geology, Institute of Earth Environment, CAS, Xi'an 710061, China

12. Zhengzhou Tourism College, Zhengzhou 451464, China;

13. College of Environment and Planning, Henan University, Key Laboratory of Geospatial  
Technology for Middle and Lower Yellow River Region, Kaifeng 475004, China

Corresponding authors:

E-mail addresses: guxh@cug.edu.cn (X. Gu) and liujy@cug.edu.cn (J. Liu).

**Abstract:** Changes in dry spell duration have been analyzed over China and worldwide. However, the asymmetric response (i.e. skewed distribution) of short- and long-duration dry spells to warming temperature and possible mechanisms remain unknown. Here, we investigate this response based on daily weather observations during the warm-rain season (May-September) over 1961-2019 from 1540 quality-controlled stations across Eastern Monsoon China (EMC). Our results show a 1°C warming in surface air temperature (SAT) and a considerable elongation of dry spells. Specifically, the regional average, maximum, and total dry spell duration over EMC increased by +7.06%, +6.17%, and +5.16%, respectively over 1961-2019. The areas in EMC with long dry spells and high SAT are also the areas that have experienced faster increases in the duration of dry spells per degree of warming. We find increases in the frequency of long-duration dry spells, but significant decreases in the frequency of short-duration dry spells. The increasing frequency of long-duration dry-spells can be explained by the slight increase in land evaporation (+1.6%/°C) over EMC and the decrease in integrated moisture vapor transport (-3.8%/°C) with warming, such that atmospheric moisture sources cannot meet the warming-induced demand, resulting in significant decreases in relative humidity (-2.4%/°C) and precipitation (-7.0%/°C). In

contrast, the decreasing frequency of short-duration dry spells during hotter warm-rain seasons occurs when the saturation vapor pressure deficit is enhanced, leading to prolonged periods where the atmosphere is replenished to necessary saturation levels for local precipitation. Relative to cold warm-rain seasons, hot warm-rain seasons with higher SAT witness cold-dry air advection in the upper level, lower convective available potential energy, and stronger vapor divergence over EMC, which tends to suppress precipitation occurrence. With future warming, the increasing frequency and duration of dry spells in the warm-rain season is likely to be conducive to the occurrence of severe droughts and heatwaves in EMC, with negative impacts on socio-economic development in China.

**Keywords:** Warming temperature; Longer-lasting; Dry spells; Warm-rain season; Eastern Monsoon China

**Highlights:**

- The regional average, maximum, and total dry spell duration over Eastern Monsoon China (EMC) have increased by +7.1%/°C, +6.2%/°C, and +5.2%/°C, respectively;
- Long (short)-duration dry spells become more (less) frequent under warming;
- Precipitation-suppressing circulation patterns and enhanced saturation vapor pressure deficit during the hotter warm-rain season tend to lengthen the duration of dry spells.

## 1. Introduction

Total precipitation during the warm-rain season (May-September) in Eastern Monsoon China

(EMC) accounts for more than 50% of total annual precipitation, and even more than 70% in many areas of EMC (Fig. S1a). EMC is an important rain-fed agricultural region in China, and the warm-rain season is the growth period for crops such as wheat and rice (Zhou and Turvey, 2014). EMC also suffers from intense heatwaves during the warm-rain season (Kong et al., 2020; Ma et al., 2017). Dry spells (i.e. consecutive dry days; Table 1) associated with high temperature (including heatwaves) in the warm-rain season are conducive to drought generation and development (Alizadeh et al., 2020; Mazdiyasni and AghaKouchak, 2015). If dry spells are prolonged during the warm-rain season and coincide with soil moisture drying (Gu et al., 2019a; Gu et al., 2019b) and heatwaves (Kong et al., 2020), they may reduce crop yields (Li et al., 2018). These detrimental impacts on crop yields are especially important as the EMC is the home to 95% of China's population and produces more than 95% of gross domestic product (Fig. S2; Gu et al., 2020). For example, in the autumn of 2019 the middle-lower reaches of the Yangtze River experienced an extremely dry period and hot-dry drought during which crop yields were notably reduced due to the soil moisture drought (Liu and Zhou, 2021; Wang and Yuan, 2021).

Given the importance of dry spells, changes in the duration and frequency of dry spells under global warming have been studied at the global scale and in various regions of the world (Breinl et al., 2020; Chaudhary et al., 2017; Cunningham, 2020; Giorgi et al., 2011; Ho et al., 2018; Wu and Yan, 2019; Ye, 2018; Ye and Fetzer, 2019; Zhang et al., 2011; Zolina et al., 2013). Globally, increases in the duration of dry spells during the late 20<sup>th</sup> century have been detected based on both observations and model simulations, and are projected to continue in the future (Giorgi et al., 2011; Li et al., 2013). However, changes in dry spells exhibit complex geographical patterns over different regions, countries, or continents. Dry spells in the United States show heterogeneous



changes in space, with increased (decreased) duration in dry spells in central-south and southwestern (north and eastern) parts of the country (Breinl et al., 2020; Groisman and Knight, 2008). Europe is dominated by decreases in the duration of dry spells, especially over Scandinavia and southern Europe (Breinl et al., 2020; Zolina et al., 2013). In contrast to Europe, dry spells have become longer across the whole of Russia (Ye and Fetzner, 2019), and the average and extreme dry spells in Russia have increased by 0.24 and 0.86 days, respectively, for every 1°C increase in temperature (Ye, 2018). In the southern hemisphere, the whole of South America is expected to experience more prolonged dry spells in the late 21st century under a high emissions scenario based on model simulations (Pascale et al., 2016). Prolonged dry spells are also projected in parts of southern Africa (Han et al., 2019). In Australia, however, unlike South America and southern Africa, dry spells have become shorter over the past six decades (Breinl et al., 2020).

Some studies have studied dry spells in monsoon regions: in West Africa, the spatio-temporal variability of dry spells is closely related to the variability of the West African monsoon (Froidurot and Diedhiou, 2017). Over central India, dry spells during the South Asian summer monsoon season have shown statistically significant increases (Singh et al., 2014). However, few studies have investigated changes in dry spells over the EMC (Li et al., 2017; Liu et al., 2015). Liu et al. (2015) found that Northeast China has witnessed increasing numbers of dry days during summer and decreasing numbers of dry days during winter. Since changes in dry spells vary by regions and seasons, it remains unclear how dry spells during the warm-rain season in EMC respond to warming temperature.

Changes in temperature show an asymmetric structure (i.e. skewed distribution) in extremely high and low quantiles: this asymmetry has been detected in some areas of Europe (Matiu et al.,

2016), and is also projected by Global Climate Models (Kodra and Ganguly, 2014). The temporal distribution of precipitation in the monsoon region is also not uniform and has a distinct asymmetric structure (Ye et al., 2017). Under high greenhouse-gas emissions, changes in future precipitation are more uneven than present-day precipitation (Pendergrass and Knutti, 2018).

Asymmetry in the response of dry spells to warming has been noted in some regions (e.g. Ye and Fetzer, 2019; Dash et al., 2009). For example, a study in India reported a significantly decreasing trend in long-duration dry spells and a significantly increasing trend in short-duration dry spells (Dash et al., 2009), while another study in Russia, on the contrary, showed an increase in long-duration dry spells (6.1% per 1°C warming), and a decrease in short-duration dry spells (Ye and Fetzer, 2019)(2.4%/°C) . However, neither of these two studies provided the exact reasons why long dry spells might become longer (or shorter) with warming.

Climate model simulations have indicated that global warming is projected to lead to an increase in globally averaged dry spell length (Giorgi et al., 2011). According to the Clausius-Clapeyron equation, the atmospheric saturated moisture content theoretically increases by 6-7%/°C. However, the global average evaporation increases by only about 2%/°C, which is significantly lower than the increase in atmospheric moisture demand (Giorgi et al., 2011; Trenberth et al., 2003). The much lower increase in evaporation thus constrains the occurrence of precipitation and consequently lengthens the duration of dry spells (Dai et al., 2018; Giorgi et al., 2011). Given the spatial variability of precipitation and surface evaporation, this globe-based explanation requires further investigation at the regional scale. A new mechanism for the increase in dry spells identified from simulated hourly precipitation in North America is the increasing magnitude of rainstorms (Dai et al., 2020). Atmospheric moisture may be consumed by 7%/°C

after each rainstorm and require a longer period to be supplemented. However, this explanation based on hourly-scale mechanisms may be challenging to verify in daily observations, because synoptic conditions dominate the formation of individual rainstorms (Dai et al., 2020). Therefore, an important aim of this study is to explore the possible mechanisms behind the response of dry spells to warming temperature over EMC.

We address the following questions in this study:

- How do dry spells during the warm-rain season change with warming temperature over EMC?
- Is there an asymmetric response of short- and long-duration dry spells to warming temperature over EMC?
- If yes, what are the possible mechanisms responsible for this asymmetry?

## **2. Data and Methods**

### **2.1 Observations**

The monsoon region over China is defined as the region where the difference between summer and winter precipitation rate exceeds 2.0 mm/day and where total summer precipitation accounts for more than 55% of annual precipitation (Wang et al., 2012; Wu et al., 2019; Zhang et al., 2018). In this study, the boundaries of EMC are obtained from Wu et al. (2019) (Fig. 1; Wu et al., 2019). A total of 2131 stations obtained from the National Meteorological Information (<http://www.nmic.cn/>) are located in the EMC. Daily precipitation, surface air temperature (SAT), and relative humidity are obtained from 1540 of those stations after applying the following quality control during 1961-2019 (Fig. 1): less than 0.5% missing data per warm-rain season (gaps in

most stations are less than 0.1%), and less than 31 missing days per warm-season (Fig. 2). The data quality was strictly controlled and homogenized. If a gap is no longer than 2 days, missing values are filled by using the mean of their adjacent values. If a gap exceeds 2 days, missing values are linearly interpolated based on neighboring stations within a 100-km radius of the target station. A 100-km radius represents a compromise between the need to obtain sufficient neighboring stations and the desire to ensure a strong correlation between target and neighbor stations (see Luo and Lau, 2018). If no neighbor stations exist around the target station, the missing values are filled using the average value of the same day over multiple years. Because most stations have no or few missing data (Fig. 2), the filled gaps have only minor impacts on the results.

## 2.2 Reanalysis data

Daily SAT (unit: °C), land evaporation (unit: mm), geopotential height (unit: mb), meridional and zonal winds (unit: mm/s), and meridional and zonal integrated vapor transport (IVT; unit: kg/(m · s)) with a resolution of  $1.25^{\circ} \times 1.25^{\circ}$  during 1961-2019 are obtained from the JRA-55 reanalysis data. The JRA-55 reanalysis data are provided by the Japan Meteorological Agency (<http://www.jma.go.jp/jma/index.html>). Daily convective available potential energy (CAPE) with a resolution of  $0.25^{\circ} \times 0.25^{\circ}$  during 1961-2019 is obtained from the European Centre for Medium-Range Weather Forecasts (ECMWF) fifth generation atmospheric reanalysis dataset (ERA5). Hourly CAPE dataset is available at <https://www.ecmwf.int/en/forecasts/dataset/ecmwf-reanalysis-v5>.

## 2.3 Definitions of dry spell indices

For station-based precipitation data, days with total precipitation exceeding or equaling 0.1 mm are considered as rainy days and precipitation is recorded. In contrast, days with total precipitation of less than 0.1 mm are recorded as dry days. Consecutive dry days (CDD) in the warm-rain season (May–September) are defined as the number of consecutive dry days (Ye, 2018). The average (ACDD) and maximum consecutive durations (MCDD) of all CDD events in a warm-rain season are estimated. The total number of dry days in a warm-rain season is defined as total dry days (TDD). More details about the four indices can be seen in Table 1.

Spearman’s rank correlation coefficient is used to detect the correlation between dry spells and SAT. To quantitatively evaluate the response rate of dry spells to warming in EMC, a linear regression model is established between dry spells and SAT (Ye, 2018). The regression coefficient indicates the response rate of dry spells to SAT, or the change rate of dry spells by SAT. The coefficient of determination ( $R^2$ ) and the corresponding significance level ( $p$  value) are used to test the goodness of fit of the linear regression model. A  $p$  value less than 0.05 indicates that the linear regression model passes the significance test.

The station-based significance (i.e. local null hypothesis) test results of the Spearman correlations and linear regression models may sometimes be inaccurate due to high spatial correlations of dry spells at these stations. In other words, there is a proportion of stations which are erroneously detected as significant ( $p < 0.05$ ), and this can be quantified using the false discovery rate (FDR) and multiple hypothesis test (Benjamini and Hochberg, 1995; Wilks, 2016). The FDR is defined as the “*expected fraction of local null hypothesis rejections that are incorrect*” (Wilks, 2006). The problem of multiplicity is solved by the field significance test, whose null

hypothesis is that all local null hypotheses are true. We assess field significance using the FDR approach proposed by Benjamini and Hochberg (1995). In this study, the field significance level is set as the same as the local hypothesis (i.e.  $p < 0.05$ ). If the local significance is at the 0.05 level of field significance, this station passes the significance test.

The Kolmogorov-Smirnov test is used to detect whether there is a difference in the probability distribution between the probability density function (PDF) or empirical cumulative distribution function (CDF) of two groups. The difference reaches a significance level based on the test statistic  $D$  and the corresponding  $p$  value (i.e.  $p < 0.05$ ).

#### 2.4 Identification of extreme dry spells over Eastern Monsoon China

To identify extreme dry spells over the whole of EMC, we first calculate the regional average of the daily precipitation series over EMC. The time-varying mean value (i.e., the multi-year mean of each day of the year) of the daily series is then subtracted from the original time series to obtain the anomaly series. The anomaly series is divided by its standard deviation to obtain the standardized time series. Three or more consecutive days with anomalies less than one standard deviation below zero are identified as an extreme dry spell in EMC (Mandke et al., 2007; Rajeevan et al., 2010; Singh et al., 2014).

### 3. Results and discussion

#### 3.1 Changes in dry spell characteristics with warming temperature

The length of dry spells during the warm-rain season in EMC indicates a clear spatial heterogeneity (Fig. S3a-c). The warm-rain season in North China has the longest ACDD, MCDD,

and TDD, reaching more than 4, 13, and 90 days, respectively. Southwest China has the shortest ACDD, MCDD, and TDD, lasting less than 2.5, 9, and 70 days, respectively. These spatial patterns are consistent with those found in previous studies (e.g. Li et al., 2017). More than 95% of stations show significant correlations ( $p < 0.05$ ) between each metric pair (of ACDD, MCDD, and TDD; Fig. S3d-f), suggesting that their responses to warming are consistent across EMC.

ACDD, MCDD, and TDD are positively correlated with SAT at all stations. The number of stations with significant correlations is the highest when considering TDD (94.55% of stations), followed by ACDD (80.13%) and MCDD (33.96%) (Fig. S4a-c), implying that there is a close relationship between dry spells and SAT. Similarly, there are 96.69%, 81.17%, and 30.45% of the stations that pass the test of the linear regression model between TDD, ACDD, and MCDD, and SAT, respectively (Fig. S4d-f). The linear regression between dry spells and SAT shows that the response of dry spells to SAT is positive in all stations (Fig. 3a-c and Fig. S4d-f). This implies that ACDD, MCDD, and TDD are increasing with SAT warming across EMC. The areas with the most pronounced increases are located in the southwestern EMC, where the duration of dry spells (i.e. ACDD, MCDD and TDD) increases by more than 20%/°C, followed by central and northern China. Increases in dry spell duration in southwestern EMC were also found in previous studies (Duan et al., 2017; Liu et al., 2014; Ren et al., 2016; Zhang et al., 2017). Ren et al. (2016) highlighted thin speeds and rising atmospheric aerosol concentrations are two key factors that lead to the decline in light and trace precipitation events, resulting in more frequent and longer-lasting dry spells. In the southwestern EMC, the decrease in moisture supply is responsible for drying (Zhang et al., 2017), and the rapid increase in the duration of dry spells during the warm-rain season indicates a rising drought risk (Bai et al., 2007; Lin et al., 2015).

Response rates of TDD to SAT linearly decrease as the length of the climatological TDD increases ( $p < 0.01$ ; Fig. 3f and Fig. S5c), suggesting that the areas in EMC with a longer climatological TDD (such as North China) show smaller increases of TDD with SAT. However, response rates of ACDD and MCDD to SAT have positive relations with their climatological duration (Fig. 3d-e and Fig. S5a-b). This means that areas with longer climatological ACDD and MCDD also have faster increase rates with SAT. Although the linear relations between the response rates of dry spells and the climatological SAT are not as strong as those between the response rates of dry spells and the climatological lengths of dry spells, we still find consistent increases in the response rates of dry spells with the climatological SAT (Fig. 3g-i and Fig. S5d-f). Note that the increases in the response rates of dry spells in areas with climatological SAT exceeding 25 °C (southeastern EMC; Fig. S1b) tend to be slow. We hypothesize that this phenomenon may relate to the peak structure between precipitation and temperature (i.e. precipitation increases with temperature up to a peak temperature, before decreasing again) which has been reported by previous studies (e.g. Wang et al., 2017). It should be noted that the relations between percentage changes of dry spells and climatological SAT are slightly nonlinear (Fig. 3g-i). This nonlinear relationship between precipitation and temperature has been explored in previous studies (Lu et al., 2015; Zhang et al., 2018). For example, Zhang et al. (2018) found that the nonlinear increasing exposure of land area to extreme precipitation occurs in warming levels above 2°C above preindustrial temperatures. Here, simply using linear relations to regress dry spells on SAT may overestimate or underestimate the response rates. Overall, in EMC and during the warm-rain season, the areas with longer length of dry spells and higher SAT exhibit stronger responses and faster increases of dry spell duration to warming temperature.



To quantitatively evaluate the response rates of dry spells to SAT across the entire EMC, the regional averages of ACDD, MCDD, and TDD are linearly regressed on regional averages of SAT (Fig. 4a-c). These linear regression models pass the goodness of fit test. Over the whole EMC, ACDD, MCDD, and TDD increased by 7.06%/°C (0.25 days/°C), 6.17%/°C (0.79 days/°C), and 5.16%/°C (4.54 days/°C), respectively.

We also calculated the 10<sup>th</sup>, 20<sup>th</sup>, ..., 95<sup>th</sup> percentiles of all CDD events in each warm-rain season during 1961-2019, and regressed them on SAT, respectively (Fig. 4d). All the percentiles of CDD events show positive responses to temperature, suggesting that CDD events are becoming longer as temperature is warming. Nevertheless, the response rates to SAT vary distinctly and exhibit an exponential distribution along with each increasing percentile (Fig. 4d). The larger the percentile, the higher the response rates per degree of SAT. This implies that responses of short- and long-duration dry spells to warming temperature may have an inconsistent behavior. We also note that the uncertainty of response rates is larger in longer-duration dry spells, because fewer CDD events are obtained as the percentile increases.

### 3.2 Responses of short- and long-duration dry spells to warming temperature

As Fig. 4d shows that changes in the duration of CDD events with warming increase for higher percentiles, we further explore changes in the occurrence of dry spells with different durations under warming temperature (Fig. 5). The occurrences of short- and long-duration CDD events exhibit clear spatial heterogeneity (Fig. S6). For example, the number of 1-day CDD events is larger in northeastern and southern EMC, while 9+days of CDD events occur more frequently in North China. Considering this spatial heterogeneity, the percentiles are also employed as the

thresholds to count the numbers of CDD events in each warm-rain season (Fig. 5c-d).

Almost all stations show negative correlations between occurrences of 1-day CDD events and SAT, meaning that the number of 1-dry-day events decreases with warming. From 1-day to 9+day CDD events, the negative correlations gradually become positive correlations (Fig. S7), so longer-duration dry-day events occur more frequently with warming. This feature is also found in the change rates of the  $n$ -day CDD events with SAT (Fig. S8). The boxplots indicate change rates and percentages of  $n$ -day CDD events with SAT (Fig. 5a-b), and their spatial distribution is shown in Fig. S8. The change rates are clearly asymmetrically distributed with the duration of dry spells. The number of  $\leq 3$ -day dry spells shows a negative response to warming temperature in most stations, while the number of  $\geq 7$  day dry spells shows a positive response. This asymmetric distribution is more pronounced in the change percentages (Fig. 5c-d). The response of occurrences of dry spells within different percentiles to warming temperature is also asymmetric, further validating the robustness of the results in Fig. 5a-b.

We select  $\leq 3$ -day (30th) and  $\geq 9$ -day (70th) CDD events as short- and long-duration dry spells, respectively, to quantify their responses to warming temperature (Fig. 6). The regional average occurrences of short- and long-duration dry spells have a significant relationship with SAT ( $p < 0.01$ ). However, their response directions are opposite. Specifically, the occurrences of short-duration dry spells in EMC decreases by 5.08/8.73%/°C (for  $\leq 3$ -day/30th percentile events), while the occurrences of long-duration dry spells increases by 15.33/7.47%/°C (for  $\geq 9$ -day/70th percentile CDD events, respectively). We conduct a sensitivity test by selecting  $\leq 20$ th (40th) and  $\geq 80$ th (60th) CDD events as short- and long-duration dry spells, and obtain consistent results (Fig. S9).

To assess the associations with warming from another viewpoint, we construct the distributions of short and long-duration dry spells under below-normal and above-normal temperature conditions, respectively. The PDF and empirical CDF of the occurrences of short- and long-duration dry spells in the ten hottest and coldest warm-rain seasons are shown in Fig. 7. The PDF and empirical CDF of the occurrences of both short- and long-duration dry spells are significantly different between the ten hottest and coldest warm-rain seasons ( $p < 0.01$ ; Fig. 7). In the ten hottest warm-rain seasons, the PDF upper tail of short-duration dry spells is significantly lower than that in the ten coldest warm-rain seasons, and its empirical CDF moves leftwards (Fig. 7a and c). The PDF and empirical CDF of long-duration dry spells in the ten hottest and coldest warm-rain seasons are exactly opposite to those of the short-duration dry spells (Fig. 7b and d). This indicates that the occurrences of short (long)-duration dry spells have significantly decreased (increase) in the ten hottest warm-rain seasons. Specifically, the average number of  $\leq 3$ -day/30th short- ( $\geq 9$ -day/70th long-) duration dry spells is 15.3/8.7d (2.5/10.1d) in the ten hottest warm-rain seasons, while the values are 18.4/11.3d (1.4/8.1d) in the ten coldest warm-rain seasons, respectively.

### 3.3 Possible mechanisms responsible for the responses of dry spells to warming temperature

Although the response of land evaporation to warming varies regionally (i.e., positive response in northeastern EMC and negative response in the other areas), the regional average land evaporation over EMC shows a weakly increasing trend ( $1.6\%/^{\circ}\text{C}$ ; Fig. 8a-b). This increasing rate of land evaporation is close to the global average ( $2.04\%/^{\circ}\text{C}$ ; Giorgi et al., 2011). Under global warming, the summer circulation and tropical Pacific atmospheric circulation tend to weaken in

the Northern Hemisphere (Coumou et al., 2015; Vecchi et al., 2006). We also detect a weakening integrated vapor moisture transport (IVT) over the EMC as SAT increases ( $-3.8\%/^{\circ}\text{C}$ ; Fig. 8c-d). The increased atmospheric moisture demand caused by increasing temperature is not mirrored by increasing land evaporation and decreasing IVT, resulting in a significant decrease in relative humidity ( $-2.4\ \%/^{\circ}\text{C}$ ; Fig. 8e-f), and thus a significant decrease in precipitation probability (fraction of precipitation days in the warm-rain season;  $7.0\%/^{\circ}\text{C}$ ; Fig. 8g-h). The decrease in precipitation probability is therefore likely to prolong the duration of dry spells.

The PDF and empirical CDF of relative humidity, saturated water vapor pressure deficit, precipitation probability, and IVT in the ten hottest and coldest warm-rain seasons over the EMC are further analyzed (Fig. 9). Substantially higher temperatures in the ten hottest warm-rain seasons in comparison with the ten coldest warm-rain seasons resulted in larger atmospheric moisture demand (Dai et al., 2020; Giorgi et al., 2011). Meanwhile, IVT is significantly weaker and saturation water vapor pressure deficit significantly greater in the ten hottest warm-rain seasons (Fig. 9a-b), resulting in a significant decrease in relative humidity (Fig. 9c). The increased saturation water vapor pressure deficit and reduced relative humidity lengthen the time required to replenish the atmospheric moisture content to reach precipitation levels (Dai et al., 2018; Giorgi et al., 2011), which inhibits precipitation occurrence and leads to a lower precipitation probability (Fig. 9d). The lower precipitation probability in the hotter warm-rain seasons compared to the colder warm-rain seasons favors the development of short-duration dry spells into long-duration dry spells (Singh et al., 2014). This leads to a greater frequency of long-duration dry spells and reduced frequency of short-duration dry spells with warming temperatures.

Precipitation during the warm-rain season in EMC is strongly influenced by the East Asian

summer monsoon. The East Asian summer monsoon has been weakening markedly in recent decades (Liu et al., 2019), which is unfavorable to precipitation occurrence. Therefore, we also analyze atmospheric circulation patterns during extreme dry spells across the entire EMC (Fig. 10), as identified by the methods in Section 2.4. During extreme dry spells in EMC, an anomalous anticyclone in the upper troposphere (200 mb) in northern Asia brings cold-dry air from the Mongolian Plateau to northern EMC, and is further advected to the southern EMC by an anomalous cyclone located in the center of EMC (Fig. 10a); CAPE in the whole EMC also significantly decreases (Fig. 10c), indicating that strong convective activity tends to be weakened. Meanwhile, the enhanced moisture divergence in the lower troposphere is also likely to suppress precipitation across EMC (Fig. 10e).

During the hot warm-rain seasons, compared with the cold warm-rain seasons, two anomalous cyclones and one anomalous anticyclone tend to occur in the upper troposphere in Central Asia, the Mongolian Plateau and the center of EMC, resulting in the advection of cold air from Central Asia (Fig. 10b). A significant reduction in CAPE (Fig. 10d) and widespread moisture divergence (although some areas in southern EMC show moisture convergence) in the lower troposphere (Fig. 10f) further tend to suppress precipitation during the hot warm-rain seasons. These circulation patterns explain the increasing duration of dry spells and greater frequency of long-duration dry spells during hot warm-rain seasons over EMC.

#### 4. Conclusions

Using *in-situ* observations across Eastern Monsoon China and reanalysis data, we investigated responses of dry spells to warming during the warm-rain season and explored

possible mechanisms behind these responses. With warming temperature, the duration of dry spells during the warm-rain season in eastern monsoon China increases significantly (5-7%/°C). The areas with long dry spells and high temperature generally show a faster increase in the duration of dry spells per degree of warming. Land evaporation increases more slowly (1.6%/°C) and integrated vapor transport decreases by 3.8%/°C, which leads to a significant decrease in relative humidity (-2.4%/°C) and precipitation probability (7.0%/°C). As a result, the duration of dry spells increases with warming temperature.

Dry spell durations do not all increase proportionally, but grow exponentially with prolonged duration. Additionally, the number of short- and long-duration dry spell events exhibits an asymmetric response to warming temperature. Specifically, hotter warm-rain seasons witness more frequent long-duration dry spell events and less frequent short-duration dry spells events over time. During the hotter warm-rain seasons, integrated vapor transport decreases in eastern monsoon China, the water vapor pressure deficit significantly increases and the relative humidity significantly decreases. The replenishment of moisture content in the atmosphere to reach levels required for precipitation would require more time, and thus inhibits the occurrence of precipitation. This mechanism tends to prolong short-duration dry spells into long-duration dry spells.

During hot warm-rain seasons, cold-dry air in upper troposphere advected from Central Asia, reduced convective effective potential energy and enhanced lower-tropospheric moisture divergence tend to suppress precipitation, resulting in longer dry spells and more frequent long-duration dry spells. Consistently, Giorgi et al. (2011) projected longer dry spells in East Asia under future warming based on model simulations. Both these projections and the increases in

long dry spells identified in our results suggest there may be rising climate-related risks of heatwaves and droughts during the warm-rain season in eastern monsoon China (Chaudhary et al., 2017; Zolina et al., 2013). Dry spells, a continuous period of dry days, can be generally taken as an indicator of drought conditions (Chaudhary et al., 2017). The increasing frequency of long dry spells in the warm-rain season is relevant information for mitigating these climate-related risks, with particular relevance for agriculture activities, water resources management, and hydrometeorological disaster prevention (Singh et al., 2014).

#### **Data available**

The station-based weather observations were obtained from the National Meteorological Information Center (<http://www.nmic.cn/>). The JRA-55 reanalysis data were obtained from the Japan Meteorological Agency (<http://www.jma.go.jp/jma/index.html>). The ERA5 CAPE data were available at <https://www.ecmwf.int/en/forecasts/dataset/ecmwf-reanalysis-v5>.

#### **Acknowledgments**

The following funding supports this study: the National Key R&D Program of China (Grant 2018YFA0605603), National Natural Science Foundation of China (Grants 41901041, U1911205, and 42001042), Central Educational Reform Fund for Colleges and Universities (2020G12), Talent Project-Scientist Program of China University of Geosciences, the Fundamental Research Funds for the Central Universities (lzujbky-2021-kb12), and Open Fund of Key Laboratory of Geospatial Technology for the Middle and Lower Yellow River Regions (Henan University), Ministry of Education (GTYR202003). We thank the editors and two reviewers for their

comments and constructive suggestions.

## References

- Alizadeh, M. R., Adamowski, J., Nikoo, M. R., AghaKouchak, A., Dennison, P., and Sadegh, M. 2020. A century of observations reveals increasing likelihood of continental-scale compound dry-hot extremes, *Science Advances*, 6(39), <https://doi.org/10.1126/sciadv.aaz4571>.
- Bai, A., Zhai, P. M., and Liu, X. D. 2007. Climatology and trends of wet spells in China, *Theoretical and Applied Climatology*, 88(3-4), 139-148, <https://doi.org/10.1007/s00704-006-0235-7>.
- Benjamini, Y., and Hochberg, Y. 1995. Controlling the false discovery rate - a practical and powerful approach to multiple testing, *Journal of the Royal Statistical Society Series B-Statistical Methodology*, 57(1), 289-300, <https://doi.org/10.1111/j.2517-6161.1995.tb02031.x>.
- Breinl, K., Di Baldassarre, G., Mazzoleni, M., Lun, D., and Vico, G. 2020. Extreme dry and wet spells face changes in their duration and timing, *Environmental Research Letters*, 15(7), <https://doi.org/10.1088/1748-9326/ab7d05>.
- Chaudhary, S., Dhanya, C. T., and Vinnarasi, R. 2017. Dry and wet spell variability during monsoon in gauge-based gridded daily precipitation datasets over India, *Journal of Hydrology*, 546, 204-218, <https://doi.org/10.1016/j.jhydrol.2017.01.023>.
- Coumou, D., Lehmann, J., and Beckmann, J. 2015. The weakening summer circulation in the northern hemisphere mid-latitudes, *Science*, 348(6232), 324-327, <https://doi.org/10.1126/science.1261768>.
- Cunningham, C. 2020. Characterization of dry spells in southeastern Brazil during the monsoon season, *International Journal of Climatology*, 40(10), 4609-4621, <https://doi.org/10.1002/joc.6478>.
- Dai, A. G., Zhao, T. B., and Chen, J. 2018. Climate change and drought: A precipitation and evaporation perspective, *Current Climate Change Reports*, 4(3), 301-312, <https://doi.org/10.1007/s40641-018-0101-6>.
- Dai, A. G., Rasmussen, R. M., Liu, C. H., Ikeda, K., and Prein, A. F. 2020. A new mechanism for warm-season precipitation response to global warming based on convection-permitting simulations, *Climate Dynamics*, 55(1-2), 343-368, <https://doi.org/10.1007/s00382-017-3787-6>.
- Dash, S. K., Kulkarni, M. A., Mohanty, U. C., and Prasad, K. 2009. Changes in the characteristics of rain events in India, *Journal of Geophysical Research-Atmospheres*, 114, <https://doi.org/10.1029/2008jd010572>.
- Duan, Y. W., Ma, Z. G., and Yang, Q. 2017. Characteristics of consecutive dry days variations in China, *Theoretical and Applied Climatology*, 130(1-2), 701-709, <https://doi.org/10.1007/s00704-016-1984-6>.
- Froidurot, S., and Diedhiou, A. 2017. Characteristics of wet and dry spells in the west African monsoon system, *Atmospheric Science Letters*, 18(3), 125-131, <https://doi.org/10.1002/asl.734>.
- Giorgi, F., Im, E. S., Coppola, E., Diffenbaugh, N. S., Gao, X. J., Mariotti, L., and Shi, Y. 2011. Higher hydroclimatic intensity with global warming, *Journal of Climate*, 24(20), 5309-5324, <https://doi.org/10.1175/2011jcli3979.1>.
- Groisman, P. Y., and Knight, R. W. 2008. Prolonged dry episodes over the conterminous United States:



461 New tendencies emerging during the last 40 years, *Journal of Climate*, 21(9), 1850-1862,  
 462 <https://doi.org/10.1175/2007jcli2013.1>.  
 463 Gu, X. H., Zhang, Q., Li, J. F., Singh, V. P., Liu, J. Y., Sun, P., and Cheng, C. X. 2019a. Attribution of  
 464 global soil moisture drying to human activities: A quantitative viewpoint, *Geophysical*  
 465 *Research Letters*, 46(5), 2573-2582, <https://doi.org/10.1029/2018gl080768>.  
 466 Gu, X. H., Zhang, Q., Li, J. F., Singh, V. P., Liu, J. Y., Sun, P., He, C. Y., and Wu, J. J. 2019b.  
 467 Intensification and expansion of soil moisture drying in warm season over Eurasia under  
 468 global warming, *Journal of Geophysical Research-Atmospheres*, 124(7), 3765-3782,  
 469 <https://doi.org/10.1029/2018jd029776>.  
 470 Gu, X. H., Zhang, Q., Li, J. F., Chen, D. L., Singh, V. P., Zhang, Y. Q., Liu, J. Y., Shen, Z. X., and Yu, H.  
 471 Q. 2020. Impacts of anthropogenic warming and uneven regional socio-economic  
 472 development on global river flood risk, *Journal of Hydrology*, 590,  
 473 <https://doi.org/10.1016/j.jhydrol.2020.125262>.  
 474 Han, F., Cook, K. H., and Vizi, E. K. 2019. Changes in intense rainfall events and dry periods across  
 475 Africa in the twenty-first century, *Climate Dynamics*, 53(5-6), 2757-2777,  
 476 <https://doi.org/10.1007/s00382-019-04653-z>.  
 477 Ho, M., Lall, U., and Cook, E. R. 2018. How wet and dry spells evolve across the conterminous United  
 478 States based on 555 years of paleoclimate data, *Journal of Climate*, 31(16), 6633-6647,  
 479 <https://doi.org/10.1175/jcli-d-18-0182.1>.  
 480 Kodra, E., and Ganguly, A. R. 2014. Asymmetry of projected increases in extreme temperature  
 481 distributions, *Scientific Reports*, 4, <https://doi.org/10.1038/srep05884>.  
 482 Kong, D. D., Gu, X. H., Li, J. F., Ren, G. Y., and Liu, J. Y. 2020. Contributions of global warming and  
 483 urbanization to the intensification of human-perceived heatwaves over China, *Journal of*  
 484 *Geophysical Research-Atmospheres*, 125(18), <https://doi.org/10.1029/2019jd032175>.  
 485 Li, J. F., Zhang, Q., Chen, Y. D., and Singh, V. P. 2013. GCMs-based spatiotemporal evolution of  
 486 climate extremes during the 21st century in China, *Journal of Geophysical*  
 487 *Research-Atmospheres*, 118(19), 11017-11035, <https://doi.org/10.1002/jgrd.50851>.  
 488 Li, J. F., Chen, Y. Q. D., Gan, T. Y., and Lau, N. C. 2018. Elevated increases in human-perceived  
 489 temperature under climate warming, *Nature Climate Change*, 8(1), 43-47,  
 490 <https://doi.org/10.1038/s41558-017-0036-2>.  
 491 Li, Z., Li, Y. P., Shi, X. P., and Li, J. J. 2017. The characteristics of wet and dry spells for the diverse  
 492 climate in China, *Global and Planetary Change*, 149, 14-19,  
 493 <https://doi.org/10.1016/j.gloplacha.2016.12.015>.  
 494 Lin, W., Wen, C., Wen, Z., and Gang, H. 2015. Drought in southwest China: A review, *Atmospheric and*  
 495 *Oceanic Science Letters*, 8(6), 339-344.  
 496 Liu, M. X., Xu, X. L., Sun, A. Y., Wang, K. L., Liu, W., and Zhang, X. Y. 2014. Is southwestern China  
 497 experiencing more frequent precipitation extremes?, *Environmental Research Letters*, 9(6),  
 498 <https://doi.org/10.1088/1748-9326/9/6/064002>.  
 499 Liu, X. D., Liu, B. H., Henderson, M., Xu, M., and Zhou, D. W. 2015. Observed changes in dry day  
 500 frequency and prolonged dry episodes in northeast China, *International Journal of Climatology*,  
 501 35(2), 196-214, <https://doi.org/10.1002/joc.3972>.  
 502 Liu, Y., et al. 2019. Anthropogenic aerosols cause recent pronounced weakening of Asian summer  
 503 monsoon relative to last four centuries, *Geophysical Research Letters*, 46(10), 5469-5479,  
 504 <https://doi.org/10.1029/2019gl082497>.

- Liu, Z., and Zhou, W. 2021. The 2019 autumn hot drought over the middle-lower reaches of the Yangtze River in China: Early propagation, process evolution, and concurrence, *Journal of Geophysical Research: Atmospheres*, 126(15), e2020JD033742, <https://doi.org/10.1029/2020JD033742>.
- Lu, E., et al. 2015. The nonlinear relationship between summer precipitation in China and the sea surface temperature in preceding seasons: A statistical demonstration, *Journal of Geophysical Research-Atmospheres*, 120(23), <https://doi.org/10.1002/2015jd024030>.
- Luo, M., and Lau, N. C. 2018. Increasing heat stress in urban areas of eastern China: Acceleration by urbanization, *Geophysical Research Letters*, 45(23), 13060-13069, <https://doi.org/10.1029/2018gl080306>.
- Ma, S. M., Zhou, T. J., Stone, D. A., Angelil, O., and Shiogama, H. 2017. Attribution of the July-August 2013 heat event in central and eastern China to anthropogenic greenhouse gas emissions, *Environmental Research Letters*, 12(5), <https://doi.org/10.1088/1748-9326/aa69d2>.
- Mandke, S. K., Sahai, A. K., Shinde, M. A., Joseph, S., and Chattopadhyay, R. 2007. Simulated changes in active/break spells during the Indian summer monsoon due to enhanced CO<sub>2</sub> concentrations: Assessment from selected coupled atmosphere-ocean global climate models, *International Journal of Climatology*, 27(7), 837-859, <https://doi.org/10.1002/joc.1440>.
- Matiu, M., Ankerst, D. P., and Menzel, A. 2016. Asymmetric trends in seasonal temperature variability in instrumental records from ten stations in Switzerland, Germany and the UK from 1864 to 2012, *International Journal of Climatology*, 36(1), 13-27, <https://doi.org/10.1002/joc.4326>.
- Mazdiyasni, O., and AghaKouchak, A. 2015. Substantial increase in concurrent droughts and heatwaves in the United States, *Proceedings of the National Academy of Sciences of the United States of America*, 112(37), 11484-11489, <https://doi.org/10.1073/pnas.1422945112>.
- Pascale, S., Lucarini, V., Feng, X., Porporato, A., and ul Hasson, S. 2016. Projected changes of rainfall seasonality and dry spells in a high greenhouse gas emissions scenario, *Climate Dynamics*, 46(3-4), 1331-1350, <https://doi.org/10.1007/s00382-015-2648-4>.
- Pendergrass, A. G., and Knutti, R. 2018. The uneven nature of daily precipitation and its change, *Geophysical Research Letters*, 45(21), 11980-11988, <https://doi.org/10.1029/2018gl080298>.
- Rajeevan, M., Gadgil, S., and Bhate, J. 2010. Active and break spells of the Indian summer monsoon, *Journal of Earth System Science*, 119(3), 229-247, <https://doi.org/10.1007/s12040-010-0019-4>.
- Ren, G. Y., et al. 2016. Spatial and temporal patterns of precipitation variability over mainland China: III: Causes for recent trends, *Advances in Water Science*, 27(3), 327-348.
- Singh, D., Tsiang, M., Rajaratnam, B., and Diffenbaugh, N. S. 2014. Observed changes in extreme wet and dry spells during the south Asian summer monsoon season, *Nature Climate Change*, 4(6), 456-461, <https://doi.org/10.1038/nclimate2208>.
- Trenberth, K. E., Dai, A., Rasmussen, R. M., and Parsons, D. B. 2003. The changing character of precipitation, *Bulletin of the American Meteorological Society*, 84(9), 1205-1217, <https://doi.org/10.1175/bams-84-9-1205>.
- Vecchi, G. A., Soden, B. J., Wittenberg, A. T., Held, I. M., Leetmaa, A., and Harrison, M. J. 2006. Weakening of tropical pacific atmospheric circulation due to anthropogenic forcing, *Nature*, 441(7089), 73-76, <https://doi.org/10.1038/nature04744>.
- Wang, B., Liu, J., Kim, H. J., Webster, P. J., and Yim, S. Y. 2012. Recent change of the global monsoon



precipitation (1979-2008), *Climate Dynamics*, 39(5), 1123-1135,  
<https://doi.org/10.1007/s00382-011-1266-z>.

Wang, G., Wang, D., Trenberth, K. E., Erfanian, A., Yu, M., Bosilovich, Michael G., and Parr, D. T. 2017. The peak structure and future changes of the relationships between extreme precipitation and temperature, *Nature Climate Change*, 7(4), 268-274,  
<https://doi.org/10.1038/nclimate3239>.

Wang, Y. M., and Yuan, X. 2021. Anthropogenic speeding up of south China flash droughts as exemplified by the 2019 summer-autumn transition season, *Geophysical Research Letters*, 48(9), <https://doi.org/10.1029/2020gl091901>.

Wilks, D. S. 2006. On "field significance" and the false discovery rate, *Journal of Applied Meteorology and Climatology*, 45(9), 1181-1189, <https://doi.org/10.1175/jam2404.1>.

Wilks, D. S. 2016. "The stippling shows statistically significant grid points" how research results are routinely overstated and overinterpreted, and what to do about it, *Bulletin of the American Meteorological Society*, 97(12), 2263-2273, <https://doi.org/10.1175/bams-d-15-00267.1>.

Wu, S., and Yan, X. D. 2019. Variations in droughts and wet spells and their influences in China: 1924-2013, *Theoretical and Applied Climatology*, 135(1-2), 623-631,  
<https://doi.org/10.1007/s00704-018-2405-9>.

Wu, Y. J., Ji, H. X., Wen, J. H., Wu, S. Y., Xu, M., Tagle, F., He, B., Duan, W. L., and Li, J. X. 2019. The characteristics of regional heavy precipitation events over Eastern Monsoon China during 1960-2013, *Global and Planetary Change*, 172, 414-427,  
<https://doi.org/10.1016/j.gloplacha.2018.11.001>.

Ye, H. C. 2018. Changes in duration of dry and wet spells associated with air temperatures in Russia, *Environmental Research Letters*, 13(3), <https://doi.org/10.1088/1748-9326/aaac0d>.

Ye, H. C., and Fetzer, E. J. 2019. Asymmetrical shift toward longer dry spells associated with warming temperatures during Russian summers, *Geophysical Research Letters*, 46(20), 11455-11462,  
<https://doi.org/10.1029/2019gl084748>.

Ye, H. C., Fetzer, E. J., Wong, S., Lambriksen, B. H., Wang, T., Chen, L. K., and Dang, V. 2017. More frequent showers and thunderstorm days under a warming climate: Evidence observed over northern Eurasia from 1966 to 2000, *Climate Dynamics*, 49(5-6), 1933-1944,  
<https://doi.org/10.1007/s00382-016-3412-0>.

Zhang, C., Tang, Q. H., Chen, D. L., Li, L. F., Liu, X. C., and Cui, H. J. 2017. Tracing changes in atmospheric moisture supply to the drying southwest China, *Atmospheric Chemistry and Physics*, 17(17), 10383-10393, <https://doi.org/10.5194/acp-17-10383-2017>.

Zhang, Q., Singh, V. P., Li, J. F., and Chen, X. H. 2011. Analysis of the periods of maximum consecutive wet days in China, *Journal of Geophysical Research-Atmospheres*, 116,  
<https://doi.org/10.1029/2011jd016088>.

Zhang, W. X., Zhou, T. J., Zou, L. W., Zhang, L. X., and Chen, X. L. 2018. Reduced exposure to extreme precipitation from 0.5 degrees C less warming in global land monsoon regions, *Nature Communications*, 9, <https://doi.org/10.1038/s41467-018-05633-3>.

Zhou, L., and Turvey, C. G. 2014. Climate change, adaptation and China's grain production, *China Economic Review*, 28, 72-89, <https://doi.org/10.1016/j.chieco.2014.01.001>.

Zolina, O., Simmer, C., Belyaev, K., Gulev, S. K., and Koltermann, P. 2013. Changes in the duration of European wet and dry spells during the last 60 years, *Journal of Climate*, 26(6), 2022-2047,  
<https://doi.org/10.1175/jcli-d-11-00498.1>.



Table 1 Definitions of dry spells associated indices

Variable	Abbreviation	Definition
Consecutive dry days	CDD	A day with total precipitation < 0.1 mm is defined as a dry day. Consecutive dry days in warm-rain season are defined as a CDD event.
Average consecutive dry days	ACDD	The average duration of all CDD events in a warm-rain season (units: d)
Maximum consecutive dry days	MCDD	The maximum duration of all CDD events in a warm-rain season (units: d)
Total dry days	TDD	The total number of dry days in a warm-rain season (units: d)

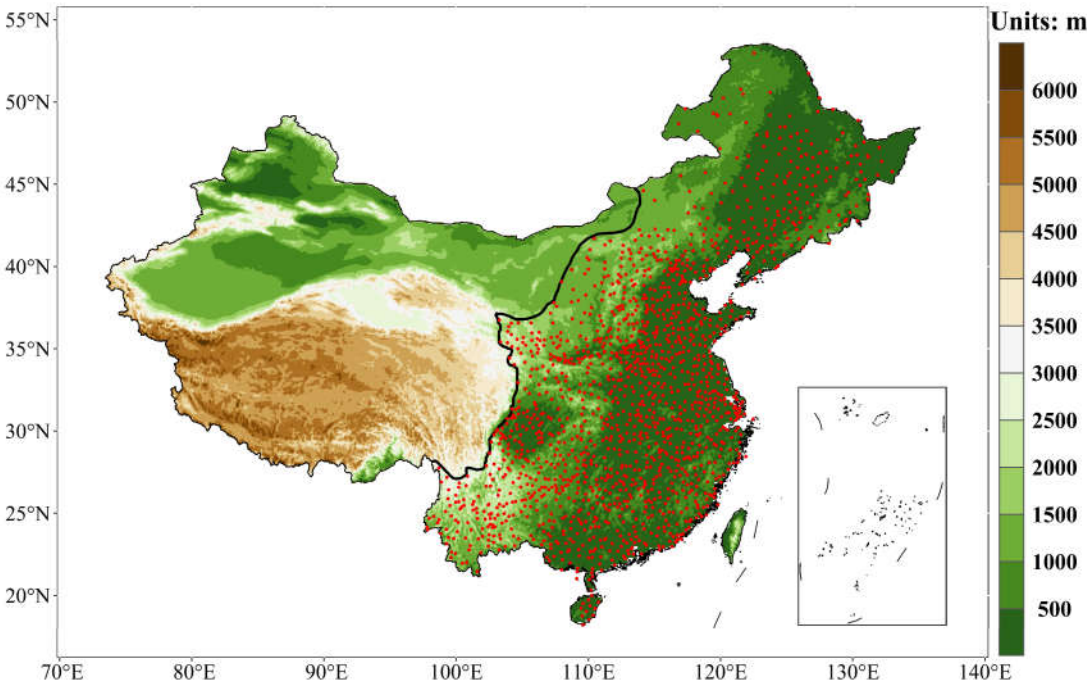


Fig. 1 Elevation and locations of weather stations (red points) over Eastern Monsoon China (EMC; delineated by the black curve).

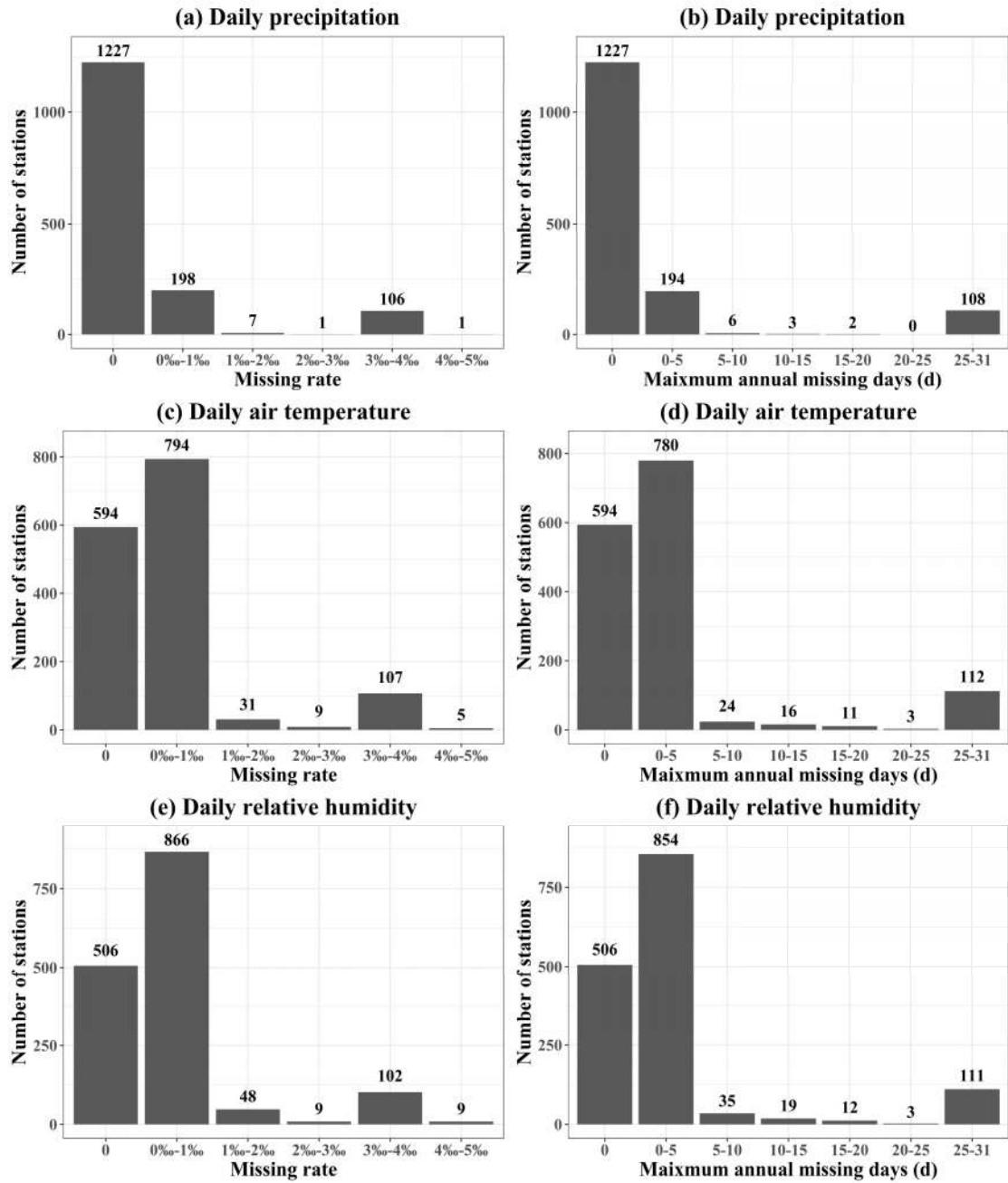


Fig. 2 Missing rate and maximum annual missing days for daily precipitation, surface air temperature (SAT), and relative humidity in the warm-rain season of 1961-2019 over EMC.



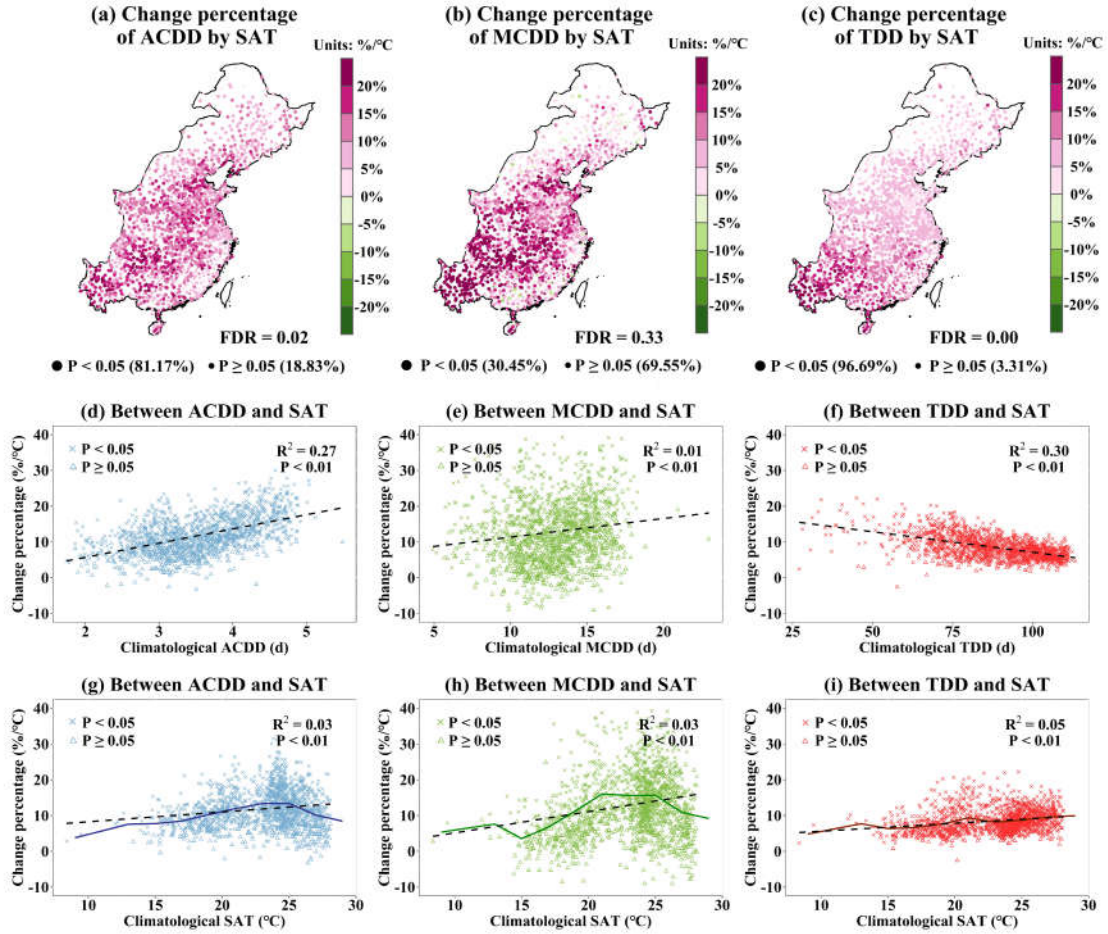


Fig. 3 Relations between average consecutive, maximum consecutive, and total dry days (ACDD, MCDD, TDD) and SAT in the warm-rain season of 1961-2019 over EMC (EMC). a-c indicate percentage change (units: %/°C) defined as the linear regression coefficients between ACDD, MCDD and TDD and SAT divided by the climatological values of ACDD, MCDD and TDD, respectively. d-i are the relations between changes of ACDD, MCDD and TDD per degree of SAT and corresponding climatological ACDD, MCDD, TDD, and SAT for all stations. Crosses (triangles) in d-i indicate relations between ACDD, MCDD and TDD and SAT that are significant (insignificant) at 95% confidence level, that is, where the  $p$  values computed for individual stations are less than (more than) 0.05 (see a-c). In a-c, the  $p$  values are at the 0.05 level of field significance after applying the false discovery rate (FDR) approach. Dashed lines are linear fitting lines for all stations;  $R^2$  is the coefficient of determination of the linear fitting line and  $p$  value is the corresponding significance. The colored solid lines in g-i are the mean values of changes of ACDD, MCDD and TDD per degree of SAT in each two-degree interval of climatological SAT (such as 10-12°C, 12-14°C, ...).



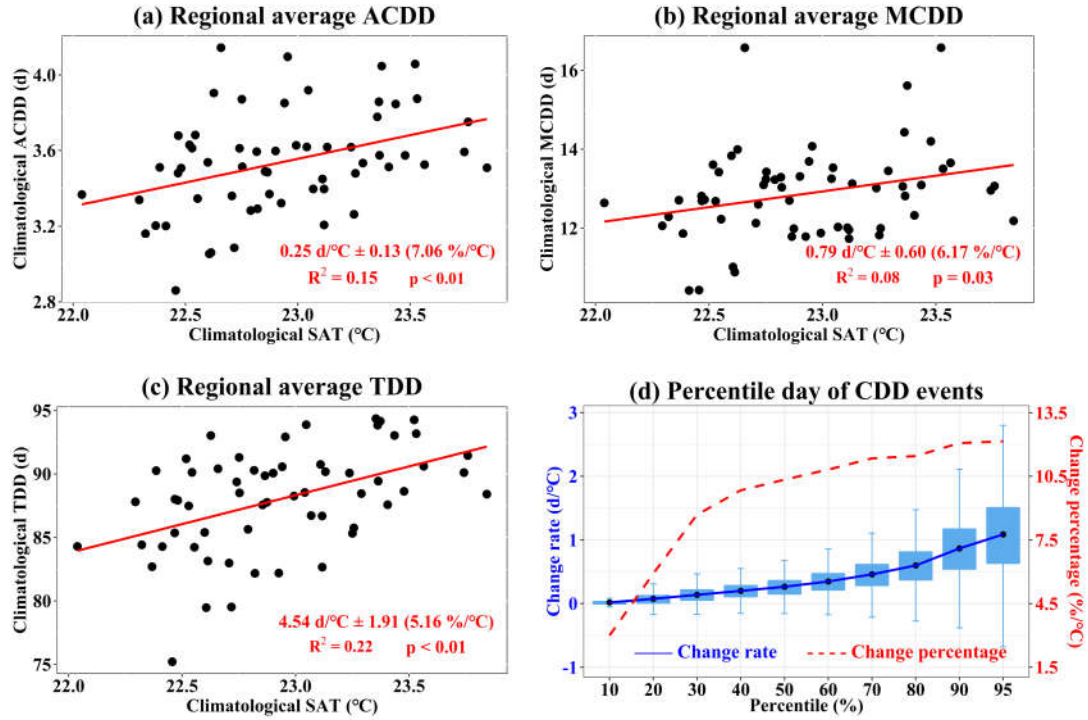


Fig. 4 Relations between regional average characteristics of dry spells and temperature. a-c, relations between regional average ACDD, MCDD and TDD and regional average SAT in the warm-rain season during 1961-2019 over EMC. d, boxplots for changes of consecutive dry days (CDD) per degree of SAT associated with different percentiles of durations. For example, the 10<sup>th</sup> percentile duration of all identified CDD events is calculated in each warm-rain season for each station, and then the time series of 10th duration is obtained. This time series is linearly regressed on SAT to compute the change rate (d/°C) and change percentage (%/°C). The same approach is applied for all percentiles. The blue dots in the boxplots indicate mean values.  $R^2$  is the determination coefficient of the linear fitting line and  $p$  value is the corresponding significance.

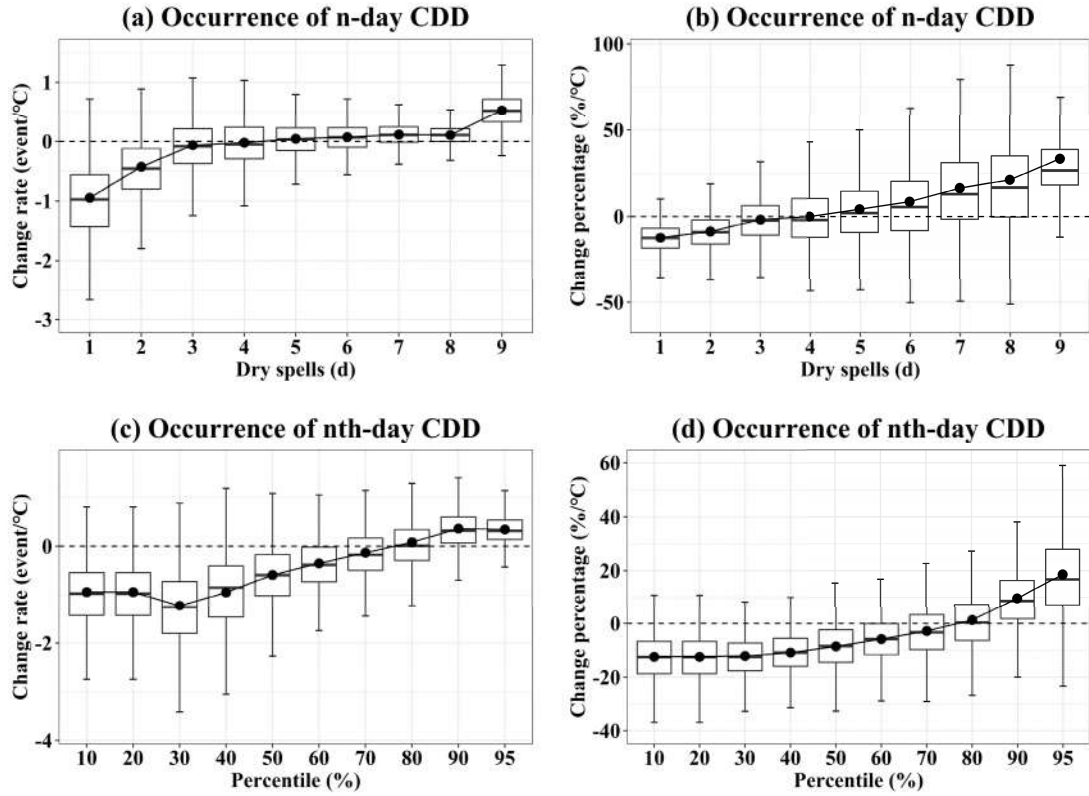


Fig. 5 Changes of CDD per degree of SAT associated with different durations and percentiles in the warm-rain season of 1961-2019 over EMC. For a and b, boxplots show the rate of change (event/°C) and percentage change (%/°C) between counts of  $n$ -day CDD events and SAT, respectively. For c and d, the 10th-95th percentile of durations of all identified CDD events in the warm-rain season of 1961-2019 for each station are taken as thresholds, and the number of CDD events with duration between each two thresholds (i.e., 0th-10th, 10th-20th, ...) are counted in each warm-rain season. This time series is linearly fitted against SAT to compute the rate of change and percentage change. The black dots in these boxplots indicate mean values.

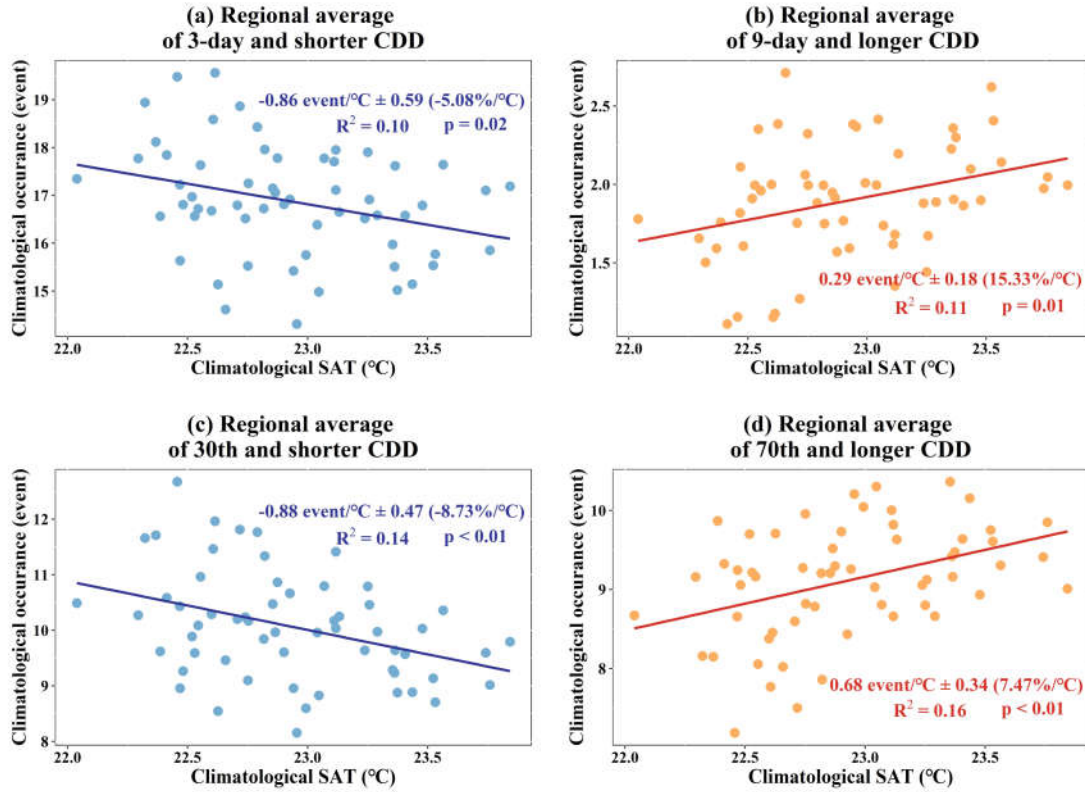


Fig. 6 Relations between regional average occurrence of short and long duration CDD and SAT in the warm-rain season of 1961-2019 over EMC. For a and b, the annual average counts of 3-day and shorter (9-day and longer) CDD are calculated in each station and then are used to compute regional means. For c and d, the 30th and 70th percentile durations of all identified CDD events in the warm-rain season of 1961-2019 for each station are taken as thresholds and then the counts below (above) 30th (70th) percentile of CDD events in each station are used to compute regional means.  $R^2$  is the coefficient of determination of the linear fitting line and the  $p$  value is the corresponding significance.

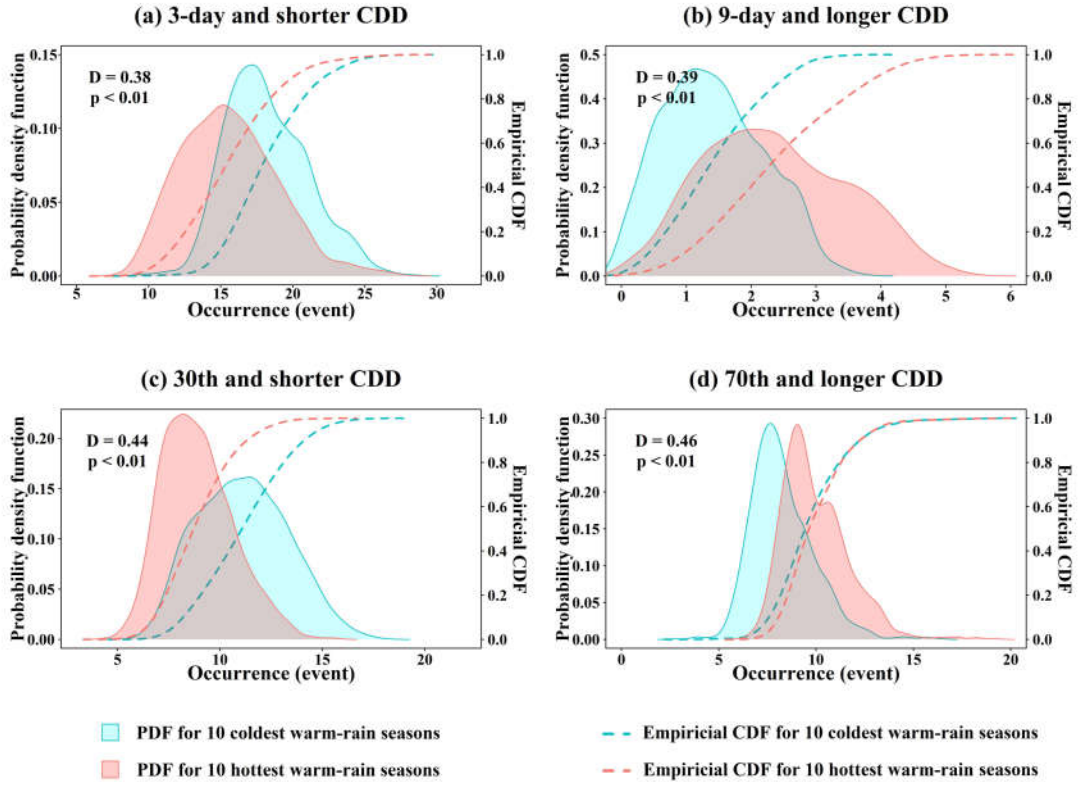


Fig. 7 Probability density function (PDF) and empirical cumulative distribution function (CDF) of occurrence of CDD events in the ten coldest and hottest warm-rain seasons of 1961-2019 over EMC. The  $D$  values on each panel are the Kolmogorov–Smirnov test statistic for the PDF difference between the ten coldest and hottest warm-rain seasons, and  $p$  values are the corresponding significances.

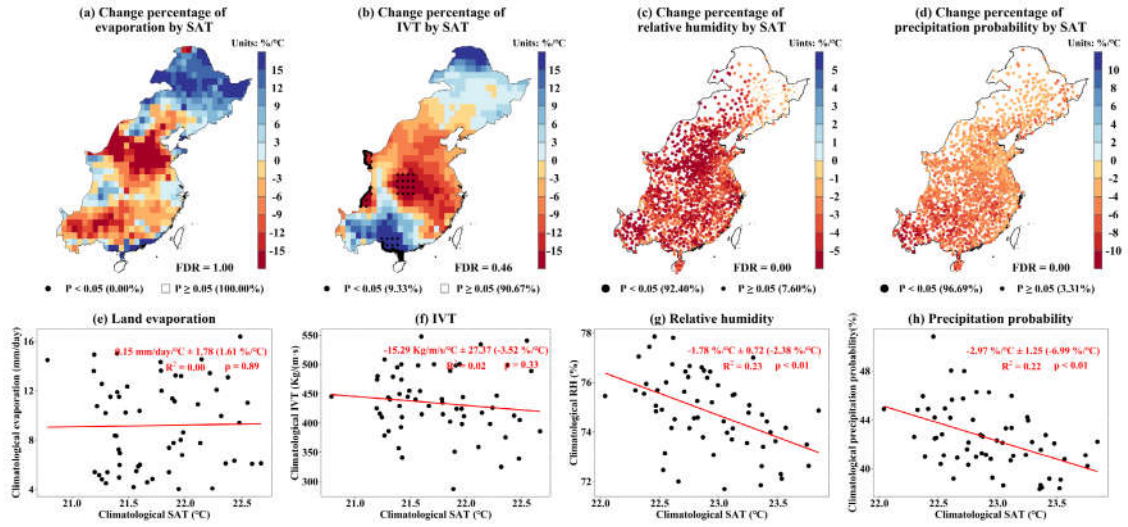


Fig. 8 Relations of evaporation, integrated vapor moisture transport (IVT), relative humidity (RH), and precipitation probability with temperature. a, b, c, and d indicate spatial distributions of percentage change (units: %/°C) in land evaporation, IVT, relative humidity, and precipitation probability per degree of SAT in the warm-rain season of 1961-2019 over EMC; e, f, g, and h are the relations between their corresponding regional averages and SAT, respectively.  $R^2$  is the coefficient of determination of the linear fitting line and  $p$  value is the corresponding significance. In a-d, the  $p$  values are at the 0.05 level of field significance using the FDR approach.

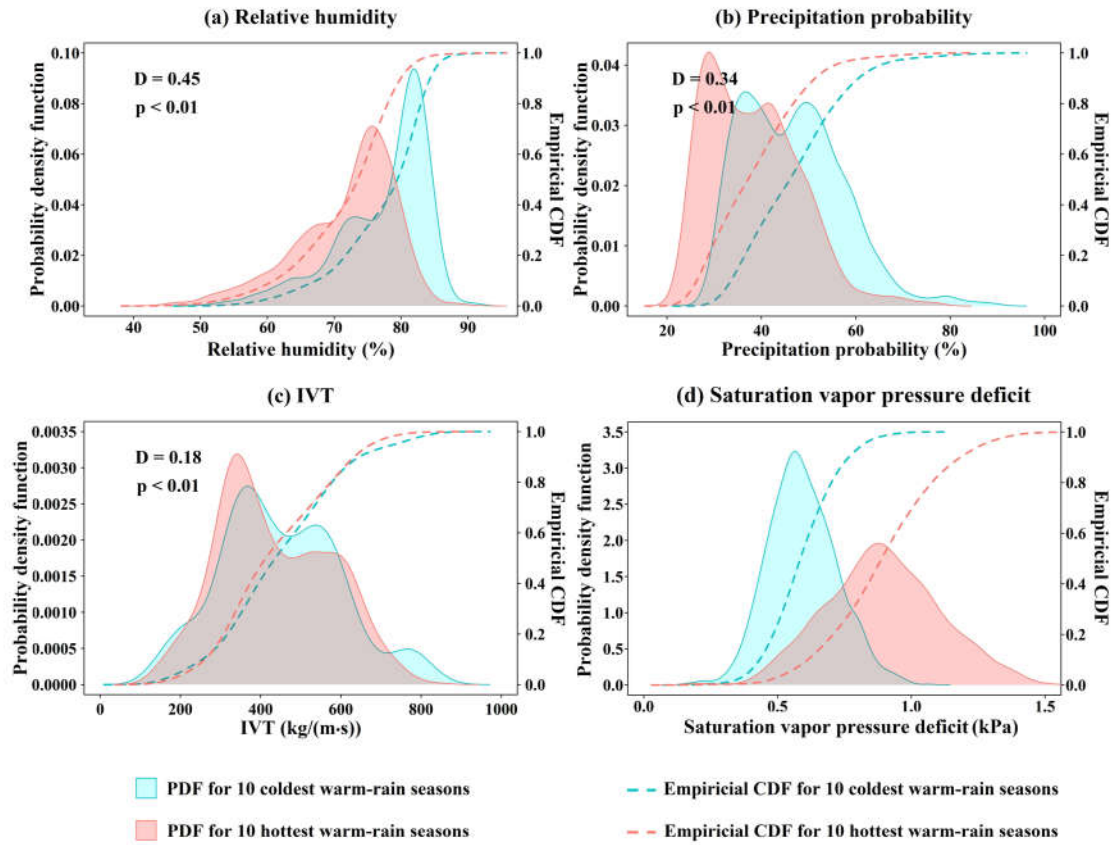


Fig. 9 The same as the Fig. 8 but for relative humidity, precipitation probability, IVT, and saturation vapor pressure deficit.



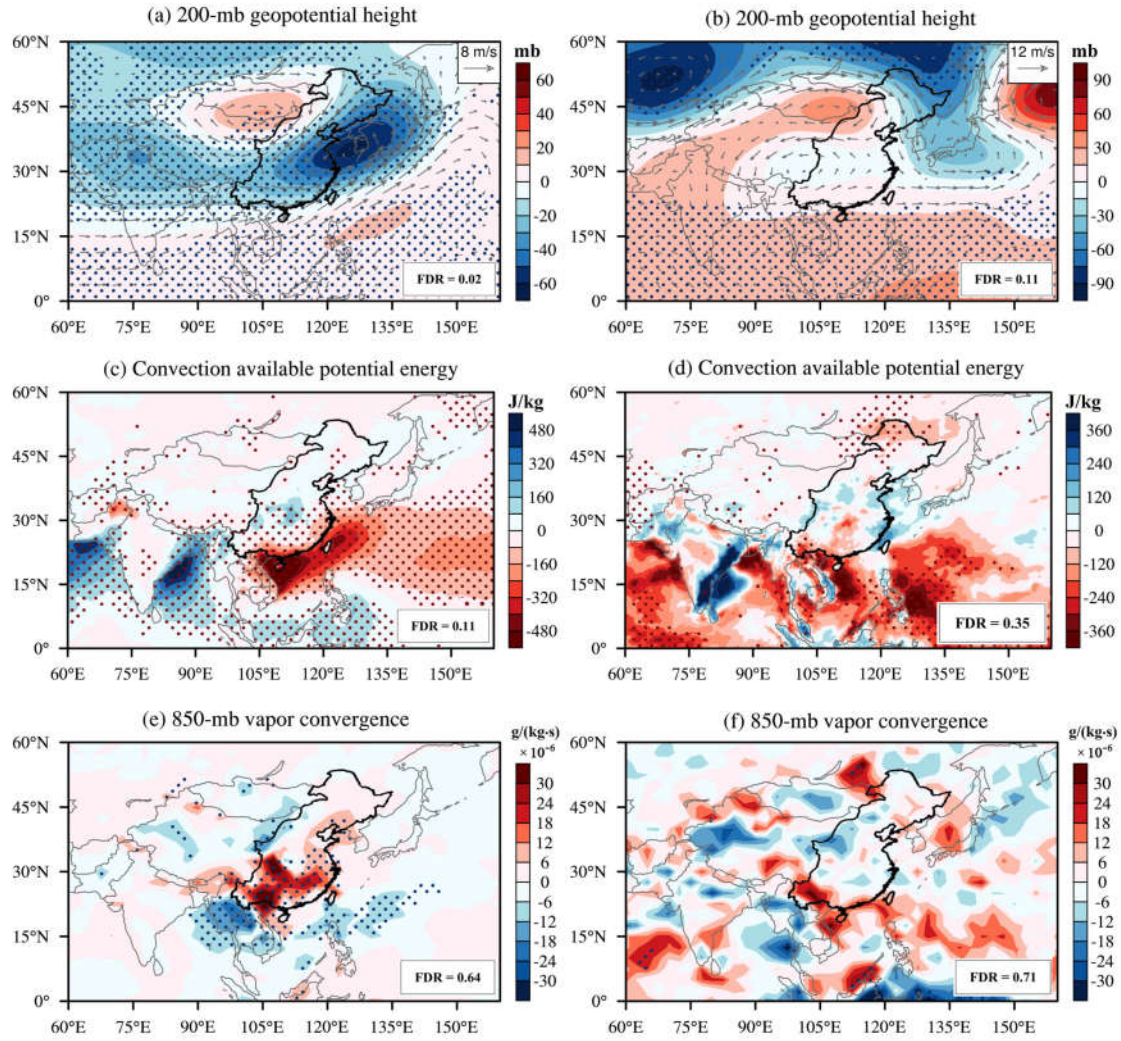


Fig. 10 Circulation patterns of dry spells in warm-rain season of 1961-2019 over EMC. a, c, and e are differences of 200-mb geopotential height and wind field, convective available potential energy (CAPE), and 850-mb vapor convergence/divergence between dry spells and the entire warm-rain season, respectively. b, d, and f are differences of 200-mb geopotential height and wind field, CAPE, and 850-mb vapor convergence/divergence during dry spells between the ten hottest and coldest warm-rain seasons, respectively. In e and f, the values above/below zero indicate vapor divergence/convergence. The colored dots in these maps indicate the differences at the 0.05 level of field significance using the FDR approach.